Cheng et al. EURASIP Journal on Wireless Communications and Networking 2013, 2013:40
http://jwcn.eurasipjournals.com/content/2013/1/40

EURASIP Journal on Wireless Communications and Networking
a SpringerOpen Journal

RESEARCH Open Access

A dimension separation-based two-dimensional correlation interferometer algorithm

Ting Cheng*, Xintao Gui and Xin Zhang

Abstract

A two-dimensional correlation interferometer algorithm based on dimension separation is proposed for wideband direction finding. The original two-dimensional angle searching is divided into 2 one-dimensional searching processes in the proposed algorithm. Therefore, the computational complexity is reduced. Meanwhile the introduced interpolation process ensures the direction finding precision. Simulation results demonstrate that compared with conventional correlation interferometer algorithm, the proposed one can offer higher direction finding speed.

Keywords: Correlation interferometer, Dimension separation, Correlation coefficient, Similarity function

1. Introduction

The information contained in the received signal of an array is commonly used to determine the incoming direction of an incident wave [1]. Such a configuration is usually called as the direction finding system. In existing direction finding systems, interferometer has the advantages of high direction finding precision, simple algorithm, and high speed, therefore, it is widely applied in military and civil fields [2,3].

Phase interferometer calculates the incoming direction with measured space phase differences between receiving elements [4]. The correlation interferometer [5,6] is the most popular one among phase interferometers. It can reduce the effect from mutual coupling and system error through comparison between measured phase difference vector and phase difference vectors in sample database [7,8]. For two-dimensional direction finding [9], the sample database consists of phase difference vectors. Each of them corresponds to a different azimuth and elevation angle pair. The number of phase difference vectors is the size of sample database, which determines the computational complexity of direction finding algorithm [10]. In order to obtain a preferable direction finding result, the size of sample database should be large enough. Therefore, the involved computational complexity grows. To the best of the authors' knowledge, the correlation interferometer algorithm based on space angle [11] is the only algorithm that dedicates to reduce the computational complexity of conventional algorithm. Although the computational complexity is reduced through introducing of two space angles, the side-effect brought to direction finding precision is not investigated.

In modern direction finding environment, there are generally more than one incoming signals. In this case, wideband direction finding system based on multi-channel structure is often adopted [12], where correlation interferometer algorithm is used to estimate the incoming direction of signal in each channel [13]. It can be seen that as the channel number grows, the involved computational complexity will increase. The real-time measuring of direction can hardly be guaranteed. To solve the problem mentioned above, a two-dimensional correlation interferometer algorithm based on new idea of dimension separation is proposed. Two different similarity functions are chosen to search for azimuth angle and elevation angle, respectively, in this algorithm. Therefore, the original two-dimensional searching is divided into 2 one-dimensional searching processes. Simulation results demonstrate the effectiveness of the proposed algorithm.

2. Problem formulation

For wideband direction finding system, the frequency range of incoming signal becomes much wider. In order to capture all possible signals, the direction finding

* Correspondence: citrus@uestc.edu.cn
School of Electronic Engineering, University of Electronic Science and Technology of China, Chengdu, Sichuan 611731, P. R. China

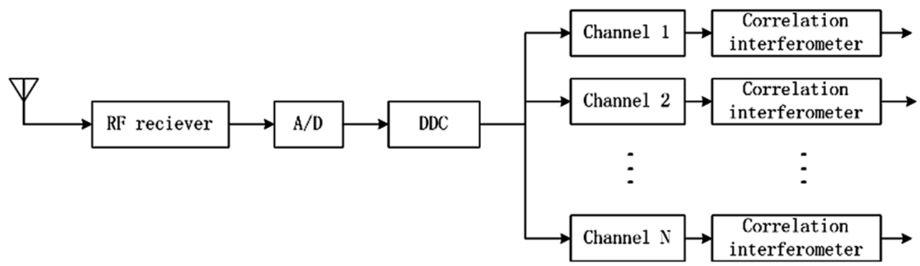

Figure 1 Structure of wideband direction finding system.

system based on multi-channel structure is always adopted. Figure 1 shows the system structure. In Figure 1, the received signal is digitalized with an A/D convertor, and then down converted with a DDC. The output of DDC is channelized into N channels. Because the incoming signal may appear in each channel, direction finding should be performed on each channel. The direction finding complexity will grow as the channel number N increases. Therefore, in order to guarantee the real-time of direction finding, it is advisable to decrease the complexity of correlation interferometer. Especially, in the two-dimensional direction finding case, where both azimuth and elevation angles should be estimated.

In two-dimensional direction finding, circular array is a commonly used array manifold. Consider an M-element uniformly spaced circular array (UCA) as shown in Figure 2, where R is the radius. The incident wave arrives with direction of (φ, θ), where φ is the azimuth angle and θ is the elevation angle. Consider the origin as the reference point, the received signal of element m can be expressed as

$$r_m(t) = A\cos(\omega_0 t - \phi_m + \phi) \tag{1}$$

where A is the amplitude, $\omega_0 = 2\pi f_0$ and f_0 is the frequency of incoming signal, the corresponding wavelength is $\lambda = c/f_0$. c represents the light speed. ϕ_m is the phase of element m relative to the reference point which can be expressed as

$$\varphi_m = \frac{2\pi R}{\lambda}\sin\theta\cos\left(\varphi - \frac{2\pi}{M}m\right) \tag{2}$$

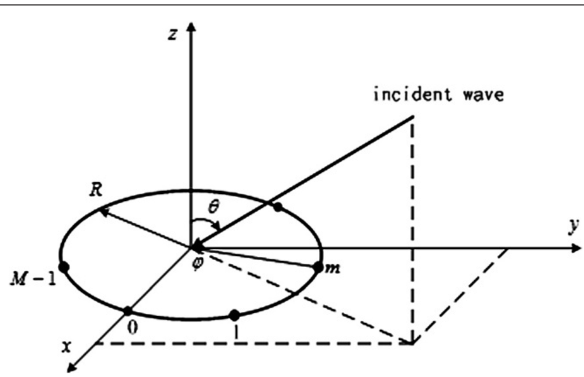

Figure 2 Array and signal model.

According to Figure 1, after frequency mixing in RF receiver, A/D sampling and digital down-conversion, the output of DDC can be expressed as

$$x_m(n) = Ae^{j[(\omega_0-\omega_1)nT_s+\phi-\phi_m]} \tag{3}$$

where T_s is the sampling interval after DDC, ω_1 is a angle frequency that determined jointly by local oscillators in RF receiver and DDC. Assume $\Delta = (\omega_0 - \omega_1)T_s = 2\pi\mu/D$, then:

$$x_m(n) = Ae^{j[\Delta n+\phi-\phi_m]} \tag{4}$$

where D is the decimator factor. When it is input into the multi-channel structure, it is filtered with a channelized filter bank. The output of channel k is

$$y_{mk}(i) = \left\{x_m(n)e^{-j\omega_k n}*h(n)\right\}_{n=iD} \tag{5}$$

where $h(n)$ is the original low-pass filter of channelized filter bank with order P, $\omega_k = 2\pi k/D$. According to (4), we have

$$y_{mk}(i) = Ae^{j[\phi+\Delta iD-\varphi_m]}\sum_{p=0}^{P-1} h(p)e^{-j(\Delta-\omega_k)p} \tag{6}$$

Once $y_{mk}(i)$ and $y_{mk}(i)$ are obtained, we can extract the phase difference between elements m and $n(\neq m)$ according to the following operation

$$y_{mk}(i)y_{nk}^{*}(i) = A^2|H(\Delta-\omega_k)|^2 e^{j[\phi_n-\phi_m]} \tag{7}$$

where $H(\omega)$ is the frequency response of original low-pass filter $h(n)$. The phase difference is

$$\begin{aligned}\phi_{m,n} &= \phi_n - \phi_m \\ &= \frac{4\pi R}{\lambda}\sin\left(\frac{\pi(n-m)}{M}\right)\sin\theta\sin\left(\varphi - \frac{\pi(n+m)}{M}\right)\end{aligned} \tag{8}$$

It can be seen in (8) that the direction of incident wave resides in the phase differences between elements. Ideally, the incoming direction of incident signal can be determined by any phase difference pair through finding the solution to two equations similar to (8). However, because of the received noise, mutual coupling or system error, different direction finding results will be obtained when using different phase difference pairs. The faced problem thus is how to determine the unique direction of incident wave according to several measured phase differences precisely.

3. Conventional two-dimensional correlation interferometer

The phase differences between different elements can form a phase difference vector. Correlation interferometer determines the incoming direction of signal through the comparison of measured phase difference vector and the vectors in sample database. Assume the interested azimuth range is $[\varphi_{\min}, \varphi_{\max}]$ and the interested elevation range is $[\theta_{\min}, \theta_{\max}]$. Divide the azimuth range with $\Delta\varphi$ and the elevation range with $\Delta\theta$, which results in P azimuth angle values and Q elevation angle values. $P \times Q$ elevation and azimuth pair can be formed. The phase difference vectors corresponding to each angle pair formulate the sample database. Obviously, the size of sample database is $P \times Q$.

Denote the measured phase difference vector as $\widetilde{\Phi}\in R^{N\times 1}$ and the ith phase difference vector in database as $\mathbf{\Phi}(i) \in R^{N\times 1}$, where N is the element number in phase difference vector. The correlation process aims to find the phase vector that most similar with the measured vector in the sample database. The angle pair of the most similar vector is considered as the estimated incoming direction. The process can be expressed as

$$\underset{(\varphi,\theta)}{\operatorname{argmax}} \left\{ f\left[\widetilde{\Phi} - \mathbf{\Phi}(i)\right], \quad i = 1, 2, \ldots, P \times Q \right\} \tag{9}$$

where $f(\cdot)$ is a function that used to measure the similarity between measured phase difference vector and the one in database, which is called as similarity function. Solving (9) is exactly a two-dimensional searching process. It can be seen that in order to get the azimuth and elevation angles, a similarity function that is sensitive both to azimuth and elevation angles should be chosen. A cosine similarity function is proposed in [14]. It has an advantage of solving phase ambiguity. According to the cosine similarity function, the similarity between measured vector and sample i in the database is calculated as

$$f_1(i) = \sum_{n=1}^{N} \cos\left(\widetilde{\Phi}_n - \Phi_n(i)\right) \tag{10}$$

where $\widetilde{\Phi}_n$ and $\Phi_n(i)$ are the nth element in $\widetilde{\Phi}$ and $\mathbf{\Phi}(i)$. The estimated direction corresponds to the sample vector that maximizes (10).

4. A dimension separation-based two-dimensional correlation interferometer

Consider two incident signals with incident angles (φ, θ_1) and (φ, θ_2). They share the same azimuth angle but have different elevation angles. If correlation coefficient $f_2(\cdot)$ is adopted as the similarity function between measured phase difference vector and sample vector, then

$$f_2^{(\varphi,\theta_1)}(i) = \frac{\widetilde{\Phi}^T(\varphi,\theta_1)\mathbf{\Phi}(i)}{\sqrt{\widetilde{\Phi}^T(\varphi,\theta_1)\widetilde{\Phi}(\varphi,\theta_1)}\sqrt{\mathbf{\Phi}^T(i)\mathbf{\Phi}(i)}} \tag{11}$$

$$f_2^{(\varphi,\theta_2)}(i) = \frac{\widetilde{\Phi}^T(\varphi,\theta_2)\mathbf{\Phi}(i)}{\sqrt{\widetilde{\Phi}^T(\varphi,\theta_2)\widetilde{\Phi}(\varphi,\theta_2)}\sqrt{\mathbf{\Phi}^T(i)\mathbf{\Phi}(i)}} \tag{12}$$

where $\widetilde{\Phi}(\varphi, \theta_i)$ represents the phase difference vector corresponds to direction of (φ, θ_i), and $(\cdot)^{\mathrm{T}}$ means the transposition operation. According to (8), it can be concluded that

$$\widetilde{\Phi}(\varphi,\theta_2) = \frac{\sin\theta_2}{\sin\theta_1}\widetilde{\Phi}(\varphi,\theta_1) \tag{13}$$

Substitute (13) into (12), we have

$$f_2^{(\varphi,\theta_2)}(i) = \frac{\frac{\sin\theta_2}{\sin\theta_1}\widetilde{\Phi}^T(\varphi,\theta_1)\mathbf{\Phi}(i)}{\sqrt{\left(\frac{\sin\theta_2}{\sin\theta_1}\right)^2\widetilde{\Phi}^T(\varphi,\theta_1)\widetilde{\Phi}(\varphi,\theta_1)}\sqrt{\mathbf{\Phi}^T(i)\mathbf{\Phi}(i)}} \tag{14}$$

Consider the common elevation range of (0°, 90°], we have $\frac{\sin\theta_2}{\sin\theta_1} > 0$ and

$$f_2^{(\varphi,\theta_1)}(i) = f_2^{(\varphi,\theta_2)}(i) \tag{15}$$

Above equation means the correlation coefficients between sample vector and measured phased difference vectors with the same azimuth are same. Accordingly, it can be concluded that the correlation coefficients between the measured phase difference vector and the vector samples with the same azimuth angle are same. Figure 3 gives an example, where the incoming direction is (105°, 40°). The measured phase difference vector is correlated with each vector sample. It can be seen from Figure 3 that the value of correlation coefficient is unchanged with elevation. Observing the sectional plan of Figure 3, the maximal value of correlation coefficient appears at the azimuth of 105° as shown in Figure 4. Because the sectional plan at different elevation remains the same as Figure 4, the azimuth can be estimated without

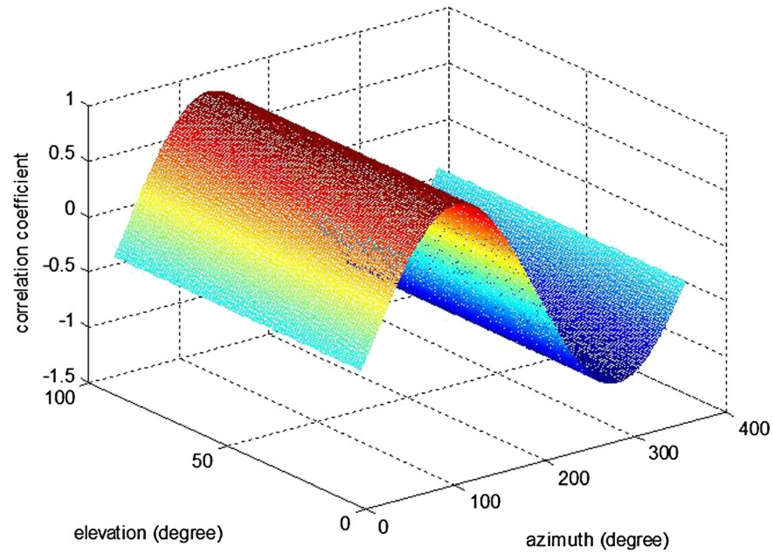

Figure 3 Correlation coefficient of measured phase difference vector with sample vector.

any information about the elevation. This phenomenon initiates the correlation interferometer based on dimension separation.

4.1 Correlation interferometer based on dimension separation

Since correlation coefficient is only relevant to azimuth angle, the conventional two-dimensional searching process can be separated. In the database, the phase difference vectors corresponding to a same elevation angle are chosen, measured phase difference vector is correlated to these sample vectors. The azimuth angle corresponding to the sample vector that maximizes the correlation coefficient can be considered as the estimated azimuth angle. Once the estimated azimuth angle is obtained, the phase difference vectors corresponding to the estimated azimuth angle are chosen. The measured phase difference vector is compared with these sample vectors where the similarity function chosen in this step should be sensitive to the elevation angle. $f_1(\cdot)$ in (10) is chosen here. The elevation angle corresponding to the sample vector that has the largest similarity is the estimated elevation angle. Obviously, conventional two-dimensional searching process is divided into 2 one-dimensional searching processes in this way.

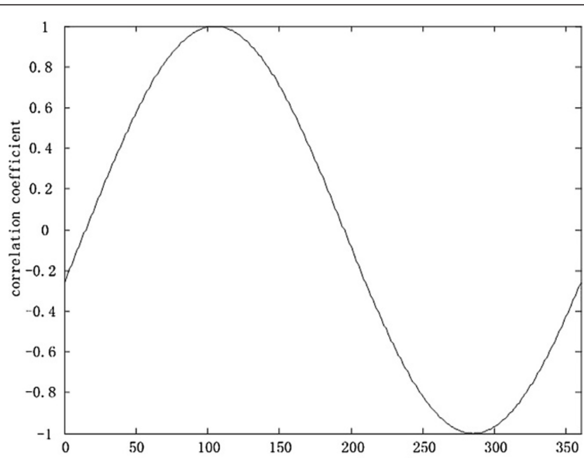

Figure 4 Sectional plan of Figure 3 at arbitrary elevation angle.

In order to increase the direction finding precision, a two-dimensional interpolation [15] is introduced after 2 one-dimensional searching processes. Remember P and Q are the number of discrete azimuth and elevation defined in Section Conventional two-dimensional correlation interferometer. Assume the index of estimated azimuth angle is p among the sequence $\{1, 2, \ldots, P\}$, and the index of estimated elevation angle is q among the sequence $\{1, 2, \ldots, Q\}$. In the sample database, the angle pairs that contiguous to the estimated angle pair are the ones with index of $(p - 1, q + 1)$, $(p, q + 1)$, $(p + 1, q + 1)$, $(p - 1, q)$, $(p + 1, q)$, $(p - 1, q - 1)$, $(p, q - 1)$, and $(p + 1, q - 1)$. Combining with the estimated angle pair, a small sample database with nine sample vectors can be formulated as shown in Figure 5, where the similarities between measured phase difference vector and the vectors in small sample database are denoted as s_i, $i = 0, 1, \ldots, 8$. They are calculated with $f_1(\cdot)$. Switch (p, q) to the origin, the index coordinates turn to be the ones in Figure 6. Perform the fitting of quadric surface $y = a_0 + a_1x + a_2y + a_3xy + a_4x^2 + a_5y^2$ with these nine points, the coefficients are calculated as follows

$$a_0 = -\frac{1}{9}s_0 + \frac{2}{9}s_1 - \frac{1}{9}s_2 + \frac{2}{9}s_3 + \frac{5}{9}s_4 + \frac{2}{9}s_5 - \frac{1}{9}s_6 + \frac{2}{9}s_7 - \frac{1}{9}s_8$$
$$a_1 = -\frac{1}{6}s_0 - \frac{1}{6}s_1 - \frac{1}{6}s_2 + \frac{1}{6}s_6 + \frac{1}{6}s_7 + \frac{1}{6}s_8$$
$$a_2 = -\frac{1}{6}s_0 + \frac{1}{6}s_2 - \frac{1}{6}s_3 + \frac{1}{6}s_5 - \frac{1}{6}s_6 + \frac{1}{6}s_8$$
$$a_3 = \frac{1}{4}s_0 - \frac{1}{4}s_2 - \frac{1}{4}s_6 + \frac{1}{4}s_8$$
$$a_4 = \frac{1}{6}s_0 + \frac{1}{6}s_1 + \frac{1}{6}s_2 - \frac{1}{3}s_3 - \frac{1}{3}s_4 - \frac{1}{3}s_5 + \frac{1}{6}s_6 + \frac{1}{6}s_7 + \frac{1}{6}s_8$$
$$a_5 = \frac{1}{6}s_0 - \frac{1}{3}s_1 + \frac{1}{6}s_2 + \frac{1}{6}s_3 - \frac{1}{3}s_4 + \frac{1}{6}s_5 + \frac{1}{6}s_6 - \frac{1}{3}s_7 + \frac{1}{6}s_8 \tag{16}$$

The coordinates of surface peak are

$$x_0 = \frac{a_2a_3 - 2a_1a_5}{4a_4a_5 - a_3^2}, \quad y_0 = \frac{a_1a_3 - 2a_2a_4}{4a_4a_5 - a_3^2} \tag{17}$$

Therefore, the azimuth and elevation angles can finally be estimated as

$$\hat{\theta} = \hat{\theta}_0 + x_0.\Delta\theta, \hat{\varphi} = \hat{\varphi}_0 + y_0.\Delta\varphi \tag{18}$$

where $\hat{\theta}_0$ and $\hat{\varphi}_0$ are the estimated azimuth and elevation angles, respectively, after 2 one-dimensional searching processes.

Based on above illustration, the two-dimensional correlation interferometer algorithm based on dimension separation can be obtained. The steps are shown as below.

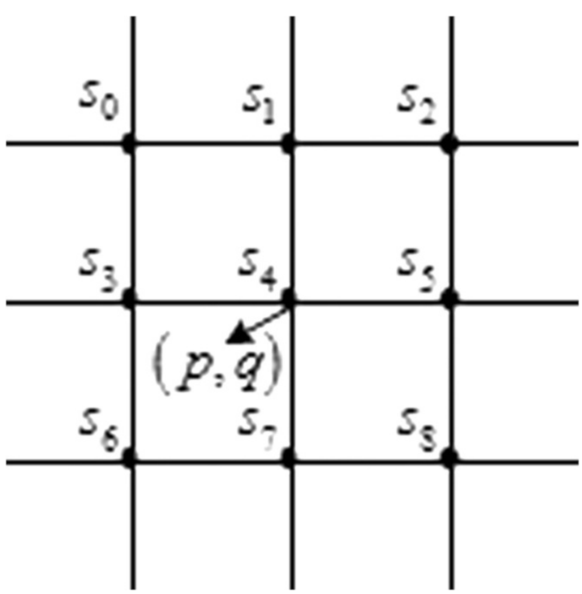

Figure 5 Diagram of small sample database.

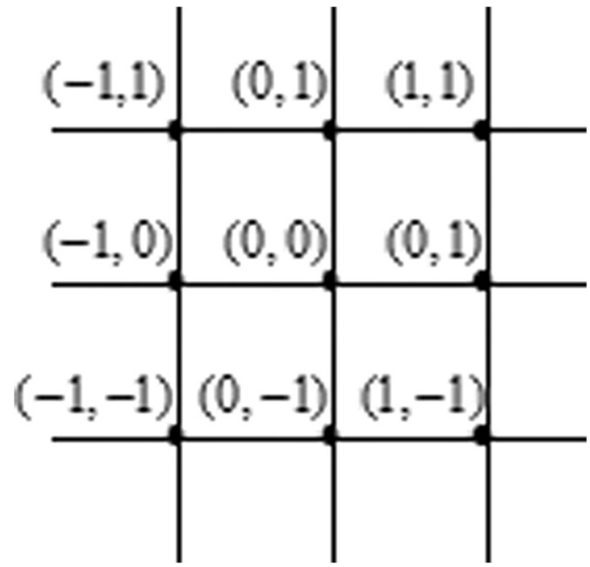

Figure 6 Result of coordinates transformation.

Step 1: Choose an arbitrary fixed elevation angle, and select all of the phase difference vectors corresponding to this elevation angle but different azimuth angles in sample database.
Step 2: Compute the correlation coefficient between measured phase difference vector and all chosen phase difference vectors in Step 1.
Step 3: Choose the azimuth angle corresponding to the phase difference vector which has the maximum correlation coefficient as estimated azimuth angle and denote it as $\hat{\phi}_0$.
Step 4: Choose all phase difference vectors which share the same azimuth angle that estimated in Step 3.
Step 5: Compute the similarity between the measured phase difference vector and all chosen phase difference vectors in Step 4 according to (10).
Step 6: Choose the elevation angle corresponding to the phase difference vector which has the maximum similarity value as estimated elevation angle and denote it as $\hat{\theta}_0$.
Step 7: Process the two-dimensional interpolation and obtain the final estimated azimuth and elevation angles according to (16)–(18).

Figure 7 shows the flow chart of above algorithm. The azimuth angle is estimated in Steps 1 to 3, where an arbitrary elevation angle is selected because the correlation coefficient is independent of it as shown in Figure 3. The following steps aim to estimate the elevation, where

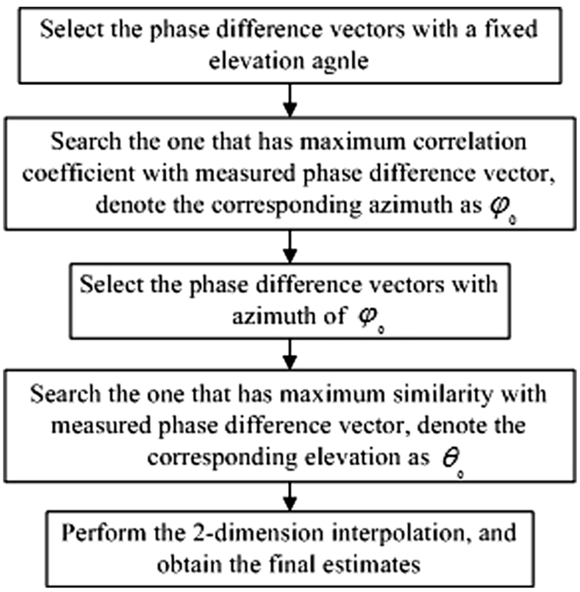

Figure 7 **Flow chart of dimension separation based correlation interferometer algorithm.**

the cosine similarity function is used for its sensitivity to the elevation angle. It is worth mentioning that if $\Delta\varphi$ and $\Delta\theta$ from the database are small enough, running from Steps 1 to 6 is enough to yield a satisfactory result. Therefore, the interpolation process can be avoided. If original sample database contains $P \times Q$ sample vectors, there are $P \times Q$ times operations that are used to compute the similarities in conventional correlation interferometer algorithm. In the correlation interferometer algorithm based on dimension separation, the involved similarity operation reduces to $P + Q$ times. The direction finding efficiency thus increases.

4.2 Condition for correlation interferometer algorithm based on dimension separation

According to the steps of correlation interferometer algorithm based on dimension separation, the key of it is the correlation coefficient which is independent on elevation angle. Therefore, the sample vectors corresponding to any elevation angle can be used for searching to give the elementary estimated azimuth angle. However, this searching process is only valid in the case of no phase ambiguity, which is also the condition for the proposed algorithm. The surface of correlation coefficient in Figure 3 will change if there is phase ambiguity. Figure 8 shows an example of correlation coefficient in the existence of phase ambiguity. The dimension separation cannot be carried out for the surface which is no longer smooth.

The condition for correlation interferometer based on dimension separation will be analyzed in the following. It is actually the condition for no phase ambiguity. The model in Section Problem Formulation ignores the effect of noise. Considering the additive noise in practical situation, the measured phase difference can be written as

$$\begin{aligned}\widetilde{\phi}_{m,n} &= \phi_{m,n} + \delta_{m,n} \\ &= \frac{4\pi R}{\lambda}\sin\left(\frac{\pi(n-m)}{M}\right)\sin\theta\sin\left(\varphi - \frac{\pi(n+m)}{M}\right) \\ &\quad + \delta_{m,n}\end{aligned} \tag{19}$$

where $\delta_{m,n}$ can be modeled as a Gaussian random variable with zero mean and variance of $\sigma^2_{m,n}$. Assume $\theta \in [\theta_L, \theta_H]$

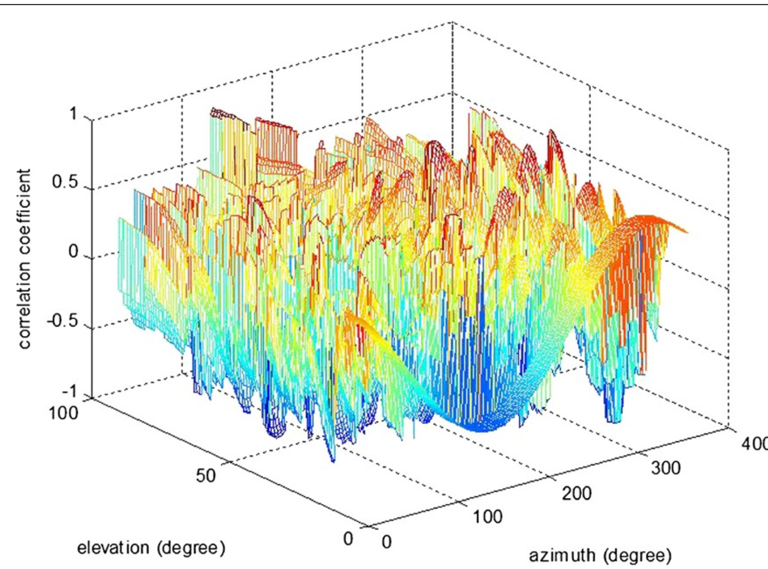

Figure 8 **Correlation coefficient surface in the existence of phase ambiguity.**

where $\sin\theta > 0$, with $n > m$ we can define a positive variable $u_{m,n} = \frac{4\pi R}{\lambda}\sin\left(\frac{\pi(n-m)}{M}\right)\sin\theta_H$. The condition for no ambiguity of $\widetilde{\phi}_{m,n}$ for any azimuth angle with probability of $1-\alpha$ can be expressed as

$$1-\alpha \le \int_{-\pi}^{\pi} p_{\widetilde{\varphi}_{m,n}}(z)dz \tag{20}$$

where

$$p_{\widetilde{\phi}_{m,n}}(z) = \frac{1}{\sqrt{2\pi\sigma_{m,n}^2}}\exp\left(-\frac{\left(z-u_{m,n}\right)^2}{2\sigma_{m,n}^2}\right) \tag{21}$$

Substitute (21) into (20), we finally have

$$1-\alpha \le F\left(\left(\pi-u_{m,n}\right)/\sigma_{m,n}\right) - F\left(-\left(\pi+u_{m,n}\right)/\sigma_{m,n}\right) \tag{22}$$

where $(x) = \int_{-\infty}^{x} \frac{1}{\sqrt{2\pi}}\exp\left(-\frac{z^2}{2}\right)dz$. For the high signal-to-noise ratio (SNR) case, $\sigma_{m,n}^2 \ll \pi^2$, (22) can be approximated as

$$1-\alpha \le F\left(\left(\pi-u_{m,n}\right)/\sigma_{m,n}\right) \tag{23}$$

Substitute the form of $u_{m,n}$ into (23), we finally have

$$\frac{R}{\lambda} \le \frac{\pi-\sigma_{m,n}.F^{-1}(1-\alpha)}{4\pi\sin\left(\frac{\pi(m-n)}{M}\right)\sin\theta_H} \tag{24}$$

Therefore, in order to use the correlation interferometer algorithm based on dimension separation, the radius to wavelength ratio must satisfy (24). For example, when $\alpha = 0.01$, $M = 9$, $R = 0.5$, $\theta_L = 0°$, $\theta_H = 90°$, the highest frequency that ensures no ambiguity between contiguous element is depicted in Figure 9 according to (24). Meanwhile, the simulated result averaged among 5,000 Monte Carlo tests is also given, where the investigated phase difference is between elements 1 and 2. It can be seen that the theoretical and simulated curves match well. According to Figure 9, when SNR is 10 dB, dimension separation is valid for signals with frequency lower than 405 MHz. Formula (24) offers the guidance of using correlation interferometer algorithm based on dimension separation in practice.

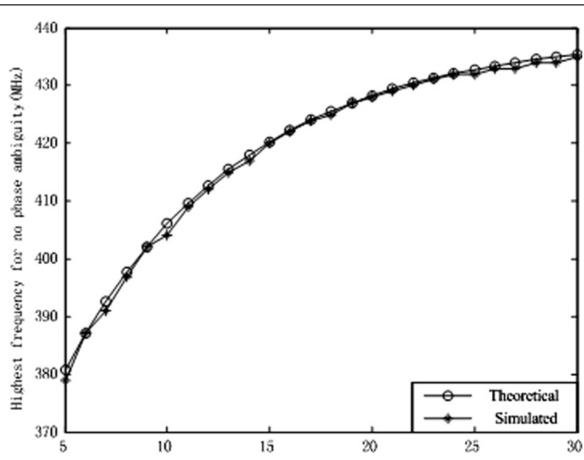

Figure 9 Highest frequency for no phase ambiguity.

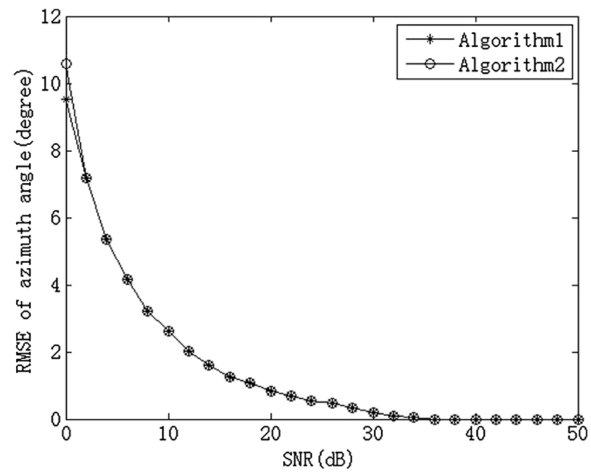

Figure 10 RMSE comparison of Algorithms 1 and 2 (azimuth angle).

5. Simulations

In this section, the dimension separation-based correlation interferometer algorithm is compared with conventional one in terms of direction finding precision and efficiency. In order to compare them in the same condition, (10) is used as the similarity function when two-dimensional searching or a searching that sensitive to elevation is involved in both algorithms. It is worth mentioning that the change of this function will not influence the comparison results. There are totally three kinds of algorithms to be compared hereinafter. They are conventional correlation interferometer algorithm, dimension separation-based correlation interferometer algorithm without interpolation and dimension separation-based correlation interferometer algorithm with interpolation. For simplicity of description, they are named as Algorithm 1 (conventional correlation interferometer algorithm), Algorithm 2 (dimension separation-based correlation interferometer algorithm without interpolation), and Algorithm 3 (dimension separation-based correlation interferometer algorithm with interpolation).

5.1 Comparison of direction finding precision

Consider a 7-element UCA with a radius of $R = 1$ m. Incidental wave arrives at the array with azimuth angle of 103°

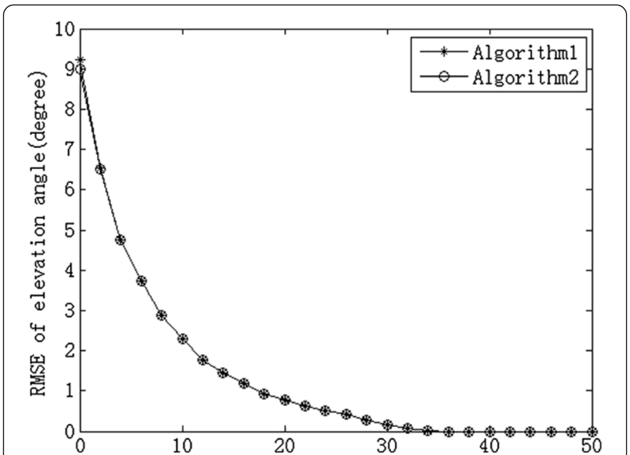

Figure 11 RMSE comparison of Algorithms 1 and 2 (elevation angle).

and elevation angle of 42°, and the carrier frequency is 70 MHz. Assume the interested azimuth and elevation ranges are [0°, 359°] and [0°, 90°], respectively, and the sample database is obtained with $\Delta\varphi = \Delta\theta = 1°$. The following results are averaged over 2,000 Monte Carlo runs. Performance of algorithms is evaluated with the root mean square error (RMSE). The average time is enough to represent the statistic characteristics of direction finding result. As $\Delta\varphi$ and $\Delta\theta$ are small, interpolation is not needed. The direction finding precisions of Algorithms 1 and 2 are compared. As mentioned before, the similarity function of (10) is used in Algorithm 1. In Algorithm 2, the correlation coefficient similarity function (11) is used first to realize dimension separation and the similarity function of (10) is used afterwards. The RMSEs of azimuth angle estimate and elevation angle estimate are shown in Figures 10 and 11. It can be seen that the precision of Algorithm 2 is

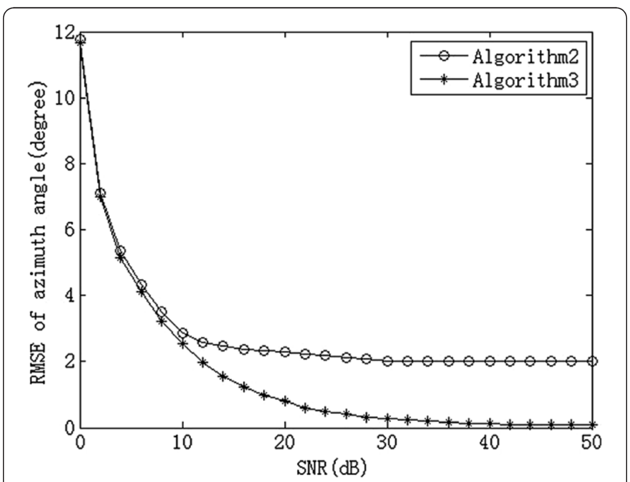

Figure 12 RMSE comparison of Algorithms 2 and 3 (azimuth angle).

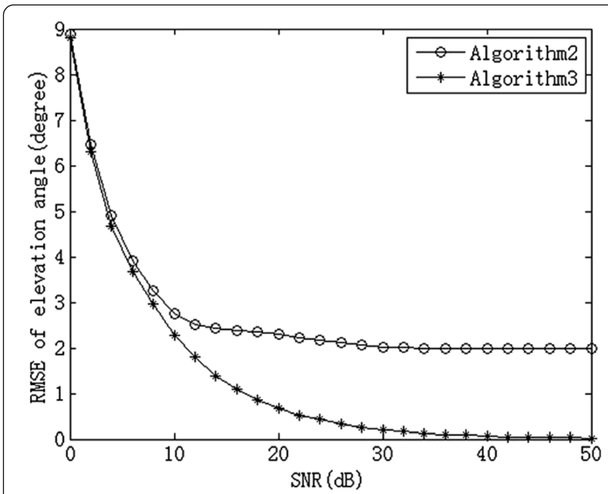

Figure 13 RMSE comparison of Algorithms 2 and 3 (elevation angle).

consistent with that of Algorithm 1. Although the complexity of Algorithm 2 is reduced compared with Algorithm 1, they offer similar direction finding precision.

In order to investigate the effect of interpolation, assume the interested azimuth and elevation ranges remain unchanged and the sample database is obtained with $\Delta\varphi = \Delta\theta = 5°$. Algorithms 2 and 3 are compared. The RMSEs of azimuth angle estimate and elevation angle estimate are shown in Figures 12 and 13. The RMSEs of azimuth and elevation estimates decrease as SNR increases. As the range of azimuth and elevation is dispersed with 5° and the real incoming angle is (103°, 42°), the RMSEs converge to 2° in Algorithm 1. However, with interpolation the RMSEs of azimuth and elevation estimates remain decrease until SNR reaches 45 dB and converge to a much smaller degree. It can be seen that with interpolation the proposed algorithm can offer higher direction finding precision. The main reason is that $\Delta\varphi$ and $\Delta\theta$ actually determines the minimum direction finding error for a given incoming direction. The interpolation process can break through the minimum error. Therefore, if $\Delta\varphi$ and $\Delta\theta$ are small, the corresponding direction finding precision is satisfactory. Algorithm 2 can be adopted. Otherwise, Algorithm 3 is a better choice.

5.2 Comparison of direction finding efficiency

In order to investigate the speed up of dimension separation, the direction finding efficiency of Algorithm 1 and the one based on dimension separation are compared. In

Table 1 $\varphi \in [0°, 359°]$, $\theta \in [0°, 90°]$ **with dispersion 1°**

Algorithm	Algorithm 1	Algorithm 2
Time (ms)	22.19240	0.12269
Speed up ratio	180.88	–

Table 2 $\varphi \in [0°, 359°]$, $\theta \in [0°, 90°]$ **with dispersion 5°**

Algorithm	Algorithm 1	Algorithm 3
Time (ms)	0.93761	0.03205
Speed up ratio	29.25	–

the CPU platform of Celeron G530 with a main frequency of 2.40 GHz, we choose C language as a programming language to investigate the average time over 10,000 runs.

Table 1 compares the direction finding efficiency when the interested azimuth and elevation ranges are [0°, 359°] and [0°, 90°], respectively, and the sample database is obtained with $\Delta\varphi = \Delta\theta = 1°$. It can be seen that Algorithm 2 needs less direction finding time and thus offers higher direction finding efficiency. The reason is that although in Algorithm 2 both similarity functions of correlation coefficient and cosine are adopted each of them is used for one dimensional searching. However, in Algorithm 1 the similarity function of cosine is used for a two-dimensional searching.

Table 2 compares the direction finding efficiency when the interested azimuth and elevation ranges are [0°, 359°] and [0°, 90°] respectively, and the sample database is obtained with $\Delta\varphi = \Delta\theta = 5°$. As $\Delta\varphi = \Delta\theta = 5°$, Algorithm 3 is used and the direction finding efficiency of it is compared with that of Algorithm 1. Similarly with the results in Table 1, Algorithm 3 consumes less direction finding time. It is worth mentioning that the efficiencies of Algorithms 2 and 3 are similar because the consumed time of interpolation is much less than that of searching process. Comparing the speed up ratio with that in Table 1, it can be seen that with the increasing of dispersion the speed up ratio will decrease accordingly. The reason is that the size of sample database will decrease when the dispersion increases.

Table 3 compares the direction finding efficiency when the interested azimuth and elevation ranges are [0°, 150°] and [0°, 70°], respectively, and the sample database is obtained with $\Delta\varphi = \Delta\theta = 1°$. Comparing the speed up ratio with the ones in Tables 1 and 2, it can be concluded that the larger the sample database, the more obvious the speed up is.

6. Conclusions

In order to increase the wideband direction finding efficiency, a two-dimensional correlation interferometer algorithm based on dimension separation is proposed. Through using correlation coefficient as a similarity function first and another similarity function that is sensitive to elevation angle later, the two-dimensional searching is separated into 2 one-dimensional searching processes. Therefore, the computational complexity is decreased. In order to guarantee the direction finding precision, a two-dimensional interpolation is introduced. Furthermore, the condition for the proposed algorithm is analyzed. Simulation results verify the effectiveness of proposed algorithm and show that the efficiency of the proposed algorithm will increase as the size of sample database grows.

Table 3 $\varphi \in [0°, 150°]$, $\theta \in [0°, 70°]$ **with dispersion 1°**

Algorithm	Algorithm 1	Algorithm 2
Time (ms)	7.31016	0.08042
Speed up ratio	90.90	–

Abbreviations
RMSE: Root mean square error; SNR: Signal-to-noise ratio.

Competing interests
The authors declare that they have no competing interests.

Acknowledgment
This study was supported by the National Natural Science Foundation of China (Grant no. 61101171).

Received: 28 November 2012 Accepted: 26 January 2013
Published: 19 February 2013

References

1. DEN Davies, Circular arrays, in *The Handbook of Antenna Design*, ed. by AW Rudge, vol. 2 (Peregrinus, London, 1983), p. 298
2. O Besson, F Vincent, P Stoica, AB Gershman, Approximate maximum likelihood estimator for array processing in multiplicative noise environments. IEEE Trans. Signal Process. **48**(9), 2506–2518 (2000). doi:10.1109/78.863054
3. M Ghogho, A Swami, TS Durrani, Frequency estimation in the presence of Doppler spread: performance analysis. IEEE Trans. Signal Process. **49**(4), 777–789 (2001). doi:10.1109/78.912922
4. G Llort-Pujol, C Sintes, X Lurton, *High-Resolution Interferometer for Multibeam Echosounders* (Oceans-Europe, Brest, France, 2005)
5. K Struckman, Correlation Interferometer geolocation, in *IEEE Antennas and Propagation Society International Symposium, 2006, Albuquerque, NM, USA*, 2006. **1**, 1141–1144, 9–14 July
6. K Pasala, R Penno, S Schneider, Novel wideband multimode hybrid interferometer system. IEEE Trans. Aerosp. Electron. Syst. **39**(4), 1396–1406 (2003). doi:10.1109/TAES.2003.1261135
7. S Henault, YMM Antar, S Rajan, R Inkol, S Wang, Impact of mutual coupling on wideband Adcock direction finders, in *Canadian Conference on Electrical and Computer Engineering, Niagara Falls, ON, Canada*, 1st edn., 2008, pp. 001327–001332. 4–7 May
8. CS Park, DY Kim, The fast correlative interferometer direction finder using I/Q demodulator, in *Asia-Pacific Conference on Communications, APCC 2006, Busan, Republic of Korea*, 1st edn., 2006, pp. 1–5. August 31–September 1
9. JL Liang, Joint Azimuth and elevation direction finding using cumulant. IEEE Sens. J. **9**(4), 390–398 (2009). doi:10.1109/JSEN.2009.2014416
10. LH Jiang, ZS He, T Cheng, KX Jia, Realization of wideband correlative interferometer algorithm based on GPU. Mod. Radar **34**(1), 35–39 (2012)
11. F Liu, W Ming, S Tao, Application of correlation operation in interferometer direction finding. Rev. Electron. Sci. Technol. **6**, 31–33 (2006)
12. B Farhang-Boroujeny, Filter bank spectrum sensing for cognitive radios. IEEE Trans. Signal Process. **56**(5), 1801–1811 (2008). doi:10.1109/TSP.2007.911490
13. YW Wu, S Rhodes, EH Satorius, Direction of arrival estimation via extended phase interferometry. IEEE Trans. Aerosp. Electron. Syst. **31**(1), 375–381 (1995). doi:10.1109/7.366318

14. HW Wei, J Wang, SF Ye, An algorithm of estimation direction of arrival for phase interferometer array using cosine function. J. Electron. Inf. Technol. **29**(11), 2665–2668 (2007)
15. L Balogh, I Kollar, Angle of arrival estimation based on interferometer principle, in *IEEE International Symposium on Intelligent Signal Processing, Budapest, Hungary*, 1st edn., 2003, pp. 219–223. 4–6 September

doi:10.1186/1687-1499-2013-40
Cite this article as: Cheng *et al.*: A dimension separation-based two-dimensional correlation interferometer algorithm. *EURASIP Journal on Wireless Communications and Networking* 2013 **2013**:40.